Phase Behavior of Ternary Polymer Blends Composed of Three Miscible Binaries

G. R. Brannock and D. R. Paul*

Department of Chemical Engineering and Center for Polymer Research, The University of Texas at Austin, Austin, Texas 78712

Received February 6, 1990; Revised Manuscript Received May 18, 1990

ABSTRACT: The phase behavior of ternary polymer blends consisting of three miscible binary pairs is examined in terms of thermodynamic theories and by experiment. The local stability of these mixtures is analyzed by using the second variation of Gibbs free energy constrained by mass balance. This treatment considers copolymer systems by using a simple binary interaction model combined with the Flory–Huggins model having temperature-dependent interaction parameters and equation of state effects by using the lattice fluid theory. The predictions indicate that asymmetry in the binary interactions may lead to ternary-phase instability manifested as large decreases in the temperatures at which phase separation occurs on heating (LCST behavior) ternary compositions relative to the binaries and/or the appearance of ternary UCST behavior when none exist in the binaries. The experimentally determined phase behavior of a series of ternary blends based on styrene/maleic anhydride (SMA) copolymers, styrene/acrylonitrile (SAN) copolymers, and either poly(methyl methacrylate), poly(ethyl methacrylate), or a methyl methacrylate/acrylonitrile (MAN) copolymer is reported. In every case, each binary pair formed miscible blends because of favorable polymer–polymer interactions. Asymmetry of binary interactions can be produced by variation of copolymer *mer* content. This was found to lead to a large drop in the ternary cloud point associated with LCST behavior relative to that of the binaries for three of the ternary mixtures. UCST behavior was not observed for any of the reported blends. Ternary spinodal calculations based on previously determined Flory–Huggins interaction parameters are grossly inaccurate when the asymmetry of the binary interactions is a dominant effect, and explanations for this are given.

Introduction

As polymer blend technology becomes more sophisticated, there is growing interest in the equilibrium phase behavior of multicomponent mixtures of polymeric components. Already several reports on ternary-phase behavior have appeared in the literature.[1-9] Nearly all of these concern an interest in homogenizing two immiscible polymers by adding a third that is miscible with both. Table I summarizes some important examples that have been studied. To our knowledge, only one ternary system has been examined to data where all three binaries are reported to form miscible blends;[10] however, we can now identify numerous ternary combinations where all three binary pairs are miscible (see Table II). The fact that each binary is miscible does not guarantee that all ternary compositions will be. Just like ternary solvent/polymer/polymer mixtures, immiscibility can be driven by an asymmetry of binary interactions, the so-called $\Delta\chi$ effect.[22a,36] For ternary polymer mixtures this may manifest itself in two ways: (1) a large drop in the ternary lower critical solution temperature (LCST) relative to those of the binaries and/or (2) the appearance of upper critical solution temperature (UCST) phenomena. In the one case that has been studied experimentally,[10] the ternary cloud-point surface (associated with LCST behavior) reported appears to vary monotonically between the three binary limits. The purpose of this paper is 2-fold.

First, we examine theoretically the thermodynamic stability of multicomponent polymer mixtures in order to better understand the circumstances that can lead to their phase separation. The local analysis is presented as a second variation of the free energy constrained by mass balance.[37] With this approach the relationship between multicomponent stability and the net interaction of the binary interaction model[38,39] becomes obvious.

Second, we examine experimentally the phase behavior of several ternary blends, based on three miscible binaries made possible by our recent observations[38] that poly(methyl methacrylate) (PMMA) and poly(ethyl methacrylate) (PEMA) form miscible blends with styrene/maleic anhydride copolymers (SMA) over certain ranges of copolymer compositions. Of course, it is well-known that PMMA and PEMA form miscible blends with styrene/acrylonitrile copolymers (SAN) over certain ranges of copolymer compositions[22a] and that SAN copolymers form miscible blends with SMA copolymers within certain ranges of AN and MA contents.[40] Thus, a multitude of ternary blends, all having miscible binaries, can be formed from PMMA or PEMA with various SAN and SMA copolymers. By manipulating *mer* content, we hoped to observe the two

Table I
Ternary Polymer Blends Having Two Miscible Binary Pairs

immiscible pair	solubilizing polymer	ref
poly(methyl methacrylate) poly(ethyl methacrylate)	poly(vinylidene fluoride)	1
poly(vinyl chloride) vinyl chloride/vinylidene chloride copolymer	nitrile butadiene rubber	2
polybutadiene polystyrene	styrene/butadiene copolymer	3
polycarbonate styrene/acrylonitrile copolymer	aliphatic polyester	4
polyarylate phenoxy	poly(ϵ-caprolactone)	5
poly(methyl methacrylate) poly(ethyl methacrylate)	styrene/acrylonitrile copolymer (or α-methylstyrene/acrylonitrile copolymer[7])	6
polycarbonate phenoxy	poly(ϵ-caprolactone)	8
polystyrene polycarbonate	tetramethyl Bisphenol A polycarbonate	9

0024-9297/90/2223-5240$02.50/0

Table II
Ternary Polymer Systems Where All Three Binaries Are Reported To Be Miscible

polymer 1	polymer 2	polymer 3	ref
bisphenol chloral polycarbonate	polycarbonate	tetramethyl polycarbonate	11–13
aliphatic polyester	polycarbonate	tetramethyl polycarbonate	13–15
aliphatic polyester	polycarbonate	vinyl chloride/vinylidene chloride copolymer	15–17
aliphatic polyester	poly(vinyl chloride)	SAN copolymer	18–20
imidized acrylic	poly(vinyl chloride)	SAN copolymer	20, 21
poly(methyl methacrylate)	poly(vinyl chloride)	SAN copolymer	21–23, 36
poly(methyl methacrylate)	poly(vinyl chloride)	α-methylstyrene/AN copolymer	23–25
poly(methyl methacrylate)	phenoxy	poly(ethylene oxide)	26–28
polyether sulfone	phenoxy	poly(ethylene oxide)	28, 29
poly(methyl acrylate)	polyepichlorohydrin	poly(ethyloxazoline)	29–31
poly(methyl acrylate)	polyepichlorohydrin	poly(ethylene oxide)	10, 32
poly(methyl acrylate)	polyepichlorohydrin	poly(vinyl acetate)	32–34
poly(ethylene oxide)	polyepichlorohydrin	poly(vinyl acetate)	10, 34, 35

Table III
Flory–Huggins Interaction Parameters

monomeric unit	S		AN		MA	
	B_{ij}^{h} [a]	B_{ij}^{s} [b]	B_{ij}^{h}	B_{ij}^{s}	B_{ij}^{h}	B_{ij}^{s}
MMA	0.181	0.0	5.00	0.0	11.68	7.85×10^{-3}
EMA	−0.245	-6.9×10^{-4}	5.33	0.0	13.40	9.91×10^{-3}
S			9.21	3.52×10^{-3}	20.43	1.83×10^{-2}
AN					−0.381	0.0

[a] In cal/cm³. [b] In cal/K·cm³.

manifestations of ternary instability mentioned above.

To help identify these possibilities, a simple Flory–Huggins type free energy expression with a temperature-dependent interaction parameter was fitted to experimental cloud-point curves and the composition limits of copolymer miscibility windows.[38] By combining this with a copolymer interaction model,[41] we were able to deduce interaction energies, $B_{ij}(T)$, for any combination of acrylonitrile, maleic anhydride, styrene, and methacrylate (MMA or EMA) monomer units in terms of a linear temperature dependence;[42] i.e.

$$B_{mn}(T) = B_{mn}^{h} - TB_{mn}^{s} \tag{1}$$

These empirical parameters (see Table III) were employed in spinodal calculations to locate unusual ternary-phase behavior for polymers composed of these monomers. Unfortunately, all of these include a binary located near a calculated spinodal divergence within the miscibility window, which may not have any physical basis. UCST behavior was predicted for some of these ternary blends, but this was not observed experimentally. In most cases, the cloud points associated with LCST behavior varied smoothly from the binary limits; however, in a few cases, a large reduction relative to binary cloud-point curves was observed.

Background and Theory

An equilibrium state is a global minimum of the free energy constrained by mass balance. Since the coexistence surface encloses the spinodal surface, which contains all locally unstable points, a spinodal analysis yields bounds on UCST and LCST behavior and is used here for simplicity. It will be shown that the addition of any number of components to an immiscible polymer pair will not homogenize the mixture unless at least one of the two polymers is present in small concentrations. Furthermore, if the combinatorial entropy is negligible, the multicomponent cloud point associated with LCST behavior is crudely bounded by those of the least stable binary when component isothermal compressibilities are similar. There is a simple thermodynamic argument for this using the Helmholtz free energy,[43] but attention will be focused here on the modified Flory–Huggins theory with a temperature-dependent interaction energy density[42] and the more realistic lattice fluid theory of Sanchez and Lacombe.[44,45] Although both theories may describe binary LCST behavior reasonably, it will be shown that their multicomponent predictions based on binary information can be quite different from each other. The same classes of phase behavior are generally described by both theories, but since enthalpic and entropic second variations are weighted differently by each, binary spinodal divergence or multicomponent UCST behavior may be predicted by one theory but not the other. The spinodal divergences of each are also qualitatively different but combinatorial entropy generally drives UCST behavior for both. General spinodal conditions will be developed next, followed by some details for each theory.

Spinodal Condition. When the second variation of the Gibbs free energy is positive in all composition directions, a phase is locally stable. Any local phase separation increases the free energy. The second variation can be written as[37]

$$\delta^2 G(\delta\phi) = \left.\frac{\partial^2 G(\phi + t\delta\phi)}{\partial t^2}\right|_{t=0} = \sum_{i=1}^{r}\sum_{j=1}^{r} G_{[ij]}\delta\phi_i\,\delta\phi_j \tag{2}$$

where ϕ_j is the volume fraction of component j, r is the number of components, $G_{[ij]} = \partial^2 G/\partial\phi_i\partial\phi_j$ with each volume fraction treated as independent, and $\delta\phi = (\delta\phi_1, \delta\phi_2, ..., \delta\phi_r)$ is the direction of the derivative. The vector $\delta\phi$ is normalized to exclude $\delta\phi = 0$ (e.g., $|\delta\phi|^2 = \sum_{i=1}^{r}(\delta\phi_i)^2 =$ constant > 0), avoiding the trivial zero $\delta^2 G(\delta\phi{=}0) = 0$, but allowed to sample all directions on the surface $\sum_{i=1}^{r}\delta\phi_i = 0$ (since $\sum_{i=1}^{r}\phi_i = 1$). With this precaution, the spinodal condition may be succinctly stated as min $\delta^2 G = 0$; the minimum value of the second variation of Gibbs free energy constrained by the normalization is zero. For a binary mixture, this reduces to

$$\begin{aligned}\min \delta^2 G(\delta\phi_1,\delta\phi_2) &= \min\{G_{[11]}(\delta\phi_1)^2 + 2G_{[12]}(\delta\phi_1)(\delta\phi_2) + G_{[22]}(\delta\phi_2)^2\}\\ &= \min\{G_{11}(\delta\phi_1)^2\}\\ &= G_{11} = 0\end{aligned} \tag{3}$$

where $G_{11} = G_{[11]} - 2G_{[12]} + G_{[22]}$ is $\partial^2 G/\partial\phi_1{}^2$ with constrained variable $\phi_2 = 1 - \phi_1$ ($\delta\phi_1 = -\delta\phi_2 \neq 0$). Similarly the multicomponent second variation may be expressed as

$$\delta^2 G(\delta\phi) = \sum_{i=1}^{r-1}\sum_{j=1}^{r-1} G_{ij}\delta\phi_i\,\delta\phi_j \tag{4}$$

where $G_{ij} = G_{[ij]} - G_{[ir]} - G_{[jr]} + G_{[rr]}$ and $\delta\phi_r =$

$-\sum_{i=1}^{r-1}\delta\phi_i$. With the elimination of the constraint $\sum_{i=1}^{r}\delta\phi_i = 0$ the quadratic form may be diagonalized into any number of convenient forms, e.g., with coefficients of determinants of diagonal submatrices, second derivatives of Legendre transforms of G, or eigenvalues of the matrix.[46] The determinant coefficients are most convenient for ternary spinodal calculations

$$G_{11} \geq 0$$

$$\det \begin{pmatrix} G_{11} & G_{12} \\ G_{12} & G_{22} \end{pmatrix} = G_{11}G_{22} - G_{12}^2 = 0 \qquad (5)$$

Flory–Huggins Theory. In this theory, the Gibbs free energy of mixing per unit volume consists of two parts: combinatorial entropy approximated by

$$\Delta S_m^{(c)} = -R\sum_{i=1}^{r}\frac{\phi_i \ln \phi_i}{V_i} \qquad (6)$$

and enthalpy given by the generalized van Laar expression

$$\Delta H_m = \sum_{i=j+1}^{r}\sum_{j=1}^{r} B_{(ij)}\phi_i\phi_j \qquad (7)$$

where V_i is the molar volume of component i and $B_{(ij)}$ is the interaction energy density between components i and j. If these components consist of several *mer* units, $B_{(ij)}$ may be expressed in terms of their interactions B_{mn}[38,39]

$$B_{(ij)} = \sum_{m>n}\sum_{n} B_{mn}(\phi_{mi} - \phi_{mj})(\phi_{nj} - \phi_{ni}) \qquad (8)$$

where ϕ_{mi} is the volume fraction of *mer* m in polymer i. When $\phi_{mi} = \phi_{mj}$ (or $\phi_{ni} = \phi_{nj}$), there is no contribution from dilution or concentration of m–n interactions.

Combinatorial entropy always favors miscibility because $-T\Delta S_m^{(c)} < 0$ and

$$-T\delta^2 S^{(c)}(\delta\phi) = RT\sum_{i=1}^{r}\eta_i(\delta\phi_i)^2 > 0 \qquad (9)$$

where $\eta_i = 1/\phi_i V_i > 0$. In the high-temperature limit, $1/T \to 0$, this becomes the dominant contribution to the free energy, but most often enthalpy determines blend miscibility. Its second variation is

$$\delta^2 H(\delta\phi) = 2\sum_{i=j+1}^{r}\sum_{j=1}^{r} B_{(ij)}\delta\phi_i\,\delta\phi_j \qquad (10)$$

An immiscible binary region, $B_{(ij)} > 0$, is propagated through most of the multicomponent phase diagram

$$\min \delta^2 G < \delta^2 G(\delta\phi_i{=}-\delta\phi_j, \delta\phi_{k\neq i,j}{=}0) = [RT(\eta_i + \eta_j) - 2B_{(ij)}](\delta\phi_i)^2 \qquad (11)$$

Only at dilute concentrations where combinatorial entropy becomes important can two polymers become solubilized.

Equation 10 is completely analogous to eq 8 with the substitution $\delta\phi_m = \phi_{mi} - \phi_{mj}$ ($\sum_m \delta\phi_m = \sum_m \phi_{mi} - \sum_m \phi_{mj} = 1 - 1 = 0$) and $-2B_{(mn)}$ replacing B_{mn}. Polymer interactions, $B_{(ij)}$, may be negative although all *mer* interactions are positive (ref 39 discusses several examples). Similarly, $\delta^2 H$ may be negative, although all $B_{(ij)}$ are negative. Assuming $|\delta^2 H| \gg |T\delta^2 S^{(c)}|$, copolymer(1–2)/homopolymer(3) miscibility results from a small deviation from regular interactions[39]

$$(B_{12})^{1/2} > (B_{13})^{1/2} + (B_{23})^{1/2} \qquad (12)$$

and similarly, even though all $B_{(ij)}$ are negative, ternary

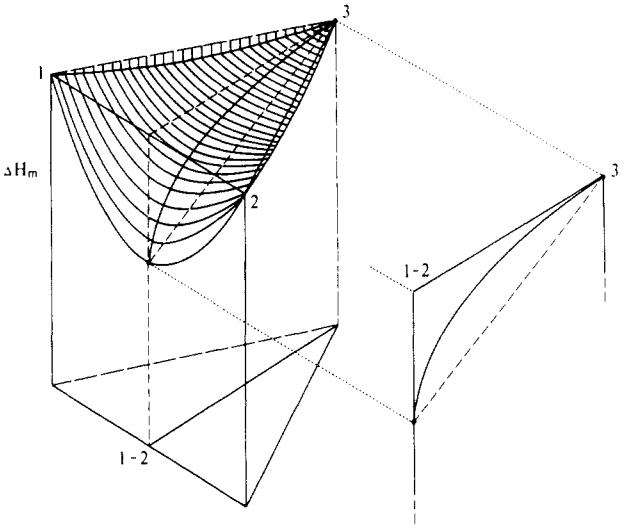

Figure 1. Simple example of ternary instability. Shown here are three binary pairs all having exothermic (convex) heats of mixing but with the 1–2 interaction being much stronger than the 1–3 and 2–3 interactions. This asymmetry can cause the ternary heat of mixing surface to form a saddle that has a concave component also (as predicted by eq 7). If the combinatorial entropy is relatively small, this will lead to a region of immisicibility within the ternary diagram. At sufficiently dilute concentrations of one or more components, ternary compositions are locally stabilized.

Table IV
Comparison of Thermodynamic Terms

term	approximate abs value, cal/cm³	term	approximate abs value, cal/cm³
$T\delta S_m^{(c)}$, $T\delta^2 S^{(c)}$	0.001–0.01	ΔH_m, $B_{(ij)} < 0$ ($B_{kl} > 0$)	0.01–0.5
$B_{kl} > 0$	0.1–10	$\delta^2 H < 0$ ($B_{(ij)} < 0$)	0.0001–0.01

instability can result when

$$(-B_{(12)})^{1/2} > (-B_{(13)})^{1/2} + (-B_{(23)})^{1/2} \qquad (13)$$

An extreme example of ternary instability is represented in Figure 1 with $B_{(12)} = -1$ and $B_{(13)} = B_{(23)} = -\epsilon$ ($0 < \epsilon \ll 1$), $1 > 2\sqrt{\epsilon}$. Here the addition of component 3 dilutes the more exothermic 1–2 random interactions as $\Delta H_m \sim (1 - \phi_3)^2 \Delta H_m(\phi_3{=}0)$, and the directional second derivative $\partial^2/\partial\phi_3{}^2 \Delta H_m|_{\phi_1/\phi_2=\text{constant}} \sim 2\Delta H_m(\phi_3{=}0)$ is negative. Although $|\delta^2 H| \gg |T\delta^2 S^{(c)}|$ is usually correct for all binary polymer pairs, it is often not for the ternary instability.

Table IV compares the approximate sizes (absolute values) of combinatorial entropy and enthalpy terms. Homopolymers of units m and n with repulsive interaction $B_{mn} > 0$ are immiscible because combinatorial entropy is negligible. Although the relative size of polymer–polymer interaction may decrease 1 or 2 orders of magnitude when miscibility is driven by a dilution of repulsive *mer* interactions $B_{(ij)} < 0$ (see eq 8), combinatorial entropy is still negligible. However, it becomes important when a local enthalpic instability, $\delta^2 H < 0$, is then created by an analogous procedure. At some reasonable temperature combinatorial entropy could induce miscibility (upper critical solution temperature, UCST, behavior). Theoretically the *mer* composition of a copolymer can be finely adjusted to produce binary UCST behavior with a homopolymer.[47] However, *mer* dispersity is a dominant factor in this region of *mer* composition, and the spinodal conditions for this mixture and the ternary discussed above are equivalent.[48]

In the Flory–Huggins model $\delta^2 G$ increases linearly with temperature for each vector $\delta\phi$ (Figure 1, diagram a); thus,

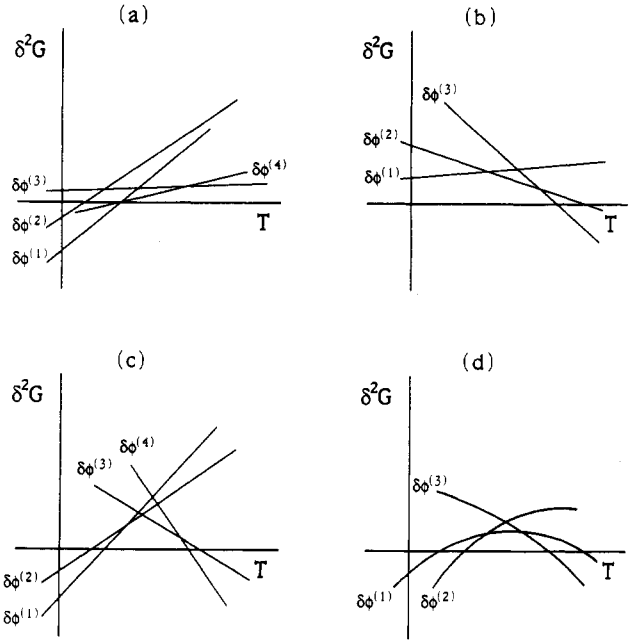

Figure 2. Location of multicomponent spinodal temperatures by minimizing the second derivative of Gibbs free energy (δ^2G) along the composition vectors $\delta\phi$: (a) describes a Flory–Huggins mixture, $B_{ij}^{h} - TB_{ij}^{s}$, with $B_{ij}^{s} = 0$; (b) and (c) have at least one $B_{ij}^{s} < 0$; and (d) represents a lattice fluid.

min δ^2G increases monotonically with temperature, implying phase homogenization on heating or USCT behavior. This is driven by enthalpy

$$\frac{\partial(\delta^2G/T)}{\partial(1/T)} = \delta^2H = T\delta^2S \leq 0 \tag{14}$$

for all linearly independent vectors $\delta\phi$ that satisfy min $\delta^2G = 0$. In contrast, phase separation on heating (LCST behavior) is driven by entropy

$$\frac{\partial(\delta^2G)}{\partial T} = -\delta^2S = -\delta^2H/T \leq 0 \tag{15}$$

for all linearly independent vectors $\delta\phi$ that satisfy min $\delta^2G = 0$. The subspace spanned by vectors for which the temperature derivative is zero requires higher order derivative conditions.

The simple Flory–Huggins theory may be modified to predict LCST behavior by adding excess entropy terms $B_{(ij)}^{s}\phi_i\phi_j$[42] to the Gibbs free energy of mixing

$$\Delta G_m = \Delta H_m - T\Delta S_m^{(e)} - T\Delta S_m^{(c)}$$
$$= \sum_{i=j+1}^{r}\sum_{j=1}^{r}(B_{(ij)}^{h} - TB_{(ij)}^{s})\phi_i\phi_j + RT\sum_{i=1}^{r}\frac{\phi_i \ln \phi_i}{V_i} \tag{16}$$

This nomenclature follows from the thermodynamic relations $\partial G/\partial T = -S$ and $\partial(G/T)/\partial(1/T) = H$ used in the previous paragraph. Again δ^2G is linear in temperature for each vector $\delta\phi$ but may increase or decrease depending on the vector and $B_{(ij)}^{s}$ terms. The three types of phase behavior that this theory predicts are shown in diagrams a–c of Figure 2. Either the mixture is miscible at all temperatures, has a UCST, is immiscible at all temperatures, has an LCST, or has both UCST and LCST. An LCST cannot occur at a lower temperature than a UCST because min δ^2G decreases at least linearly with temperature after an LCST. The general condition for LCST behavior may be restated as $\delta^2S^{(e)} > -\delta^2S^{(c)} > 0$. For a binary mixture this is $-2B_{12}^{s} > R(\eta_1 + \eta_2)$. A spinodal temperature divergence occurs whenever both sides are

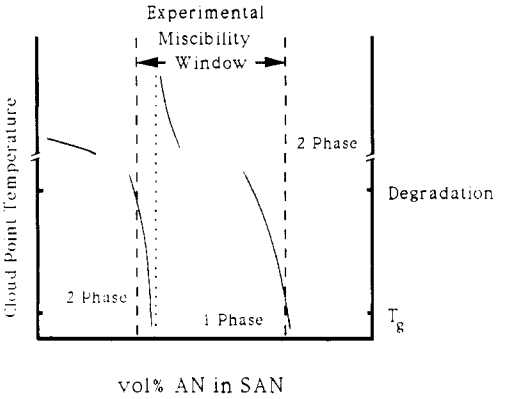

Figure 3. Schematic of spinodal divergence predicted by modified Flory–Huggins theory for SMA/SAN binary blends.

equal. This may result from the quadratic dependence of B_{12}^{s} on *mer* volume fractions ϕ_{m1} and ϕ_{n2} (eq 8) or of η_1 and η_2 on polymer volume fraction ϕ_1. Correlation of cloud points in a previous paper[38] produced the former divergence within the SMA/SAN miscibility window (Figure 3). If combinatorial entropy is negligible, min δ^2G is bounded above by the smallest binary value (substitute $B_{(ij)} = B_{(ij)}^{h} - TB_{(ij)}^{s}$ into expression 11). Therefore, multicomponent cloud-point temperatures associated with LCST behavior should be bounded by the smallest binary values. On the other hand, binary cloud-point temperatures associated with UCST behavior temperature may either decrease within the multicomponent diagram if dilution of the binary is dominant or increase if the interaction of the components is asymmetric.[3]

Lattice Fluid Theory. LCST behavior can result from chemical association[49] and specific interactions[45,50] where heat capacity destabilizes the mixture[51] or from fluid compressibility.[52] Sanchez[53] has given general arguments for the latter by expanding the density basis $\{\phi\}$ of the Gibbs free energy $G(\phi)$ to the basis $\{\phi,\tilde{\rho}\}$ of the potential $G(\phi,\tilde{\rho})$, which is equal to the free energy at its minimum

$$G_{\tilde{\rho}} = \left.\frac{\partial G}{\partial \tilde{\rho}}\right|_{T,P} = 0$$

$$G_{\tilde{\rho}\tilde{\rho}} = \left.\frac{\partial^2 G}{\partial \tilde{\rho}^2}\right|_{T,P} > 0 \tag{17}$$

where $\tilde{\rho} = \rho/\rho^*$ is a reduced density. Essentially an excess entropy term derived from lattice vacancies

$$-\frac{S^{(e)}}{k} = \frac{1-\tilde{\rho}}{\tilde{\rho}}\ln(1-\tilde{\rho}) + \frac{1}{r}\ln\tilde{\rho} \tag{18}$$

where $1/r = \sum_i(\phi_i/r_i)$ (r_i and ϕ_i are the chain length and hard-core volume fraction of polymer i, respectively) is added to a Flory–Huggins formulation of free energy.

$$H = -\tilde{\rho}\epsilon^*$$

$$\epsilon^* = \sum_{i=1}^{r}\phi_i\epsilon_{(ii)}^* - \sum_{i=j+1}^{r}\sum_{j=1}^{r}\phi_i\phi_j\Delta\epsilon_{(ij)}^*$$
$$= \sum_{i=1}^{r}\sum_{m}\phi_i\phi_{mi}\epsilon_{mm}^* - \sum_{i=1}^{r}\sum_{j=1}^{r}\sum_{m>n}\sum_{n}\phi_i\phi_{mi}\phi_j\phi_{nj}\Delta\epsilon_{mn}^*$$
$$-\frac{S^{(c)}}{k} = \sum_{i=1}^{r}\frac{\phi_i\ln\phi_i}{r_i} \tag{19}$$

Both characteristic polymer interactions $\Delta\epsilon_{(ij)}^*$ and energies $\epsilon_{(ii)}^*$ ($=E_{vap}/\tilde{\rho}r)_i$[44] contribute to the cohesiveness of the

mixture. Polymer and *mer* interactions $\Delta\epsilon_{(ij)}^*$ and $\Delta\epsilon_{mn}^*$ are related as $B_{(ij)}$ and B_{mn} are in eq 8. For an incompressible fluid ($\tilde{\rho} = 1$), $S^{(e)} = 0$ and $H = -\epsilon^*$. It is straightforward to show that $S^{(e)}$ is truly an entropy.

$$\begin{aligned} -S &= \left.\frac{\partial G}{\partial T}\right|_P \\ &= \left.\frac{\partial G}{\partial \tilde{\rho}}\right|_{T,P} \left.\frac{\partial \rho}{\partial T}\right|_P + \left.\frac{\partial G}{\partial T}\right|_{\tilde{\rho},P} \\ &= G_{\tilde{\rho}}\tilde{\rho}_T + G_T \\ &= -(S^{(c)} + S^{(e)}) \end{aligned} \tag{20}$$

The first equality is a thermodynamic relation; what follows is the use of potential G and its restriction to the thermodynamic surface $G_{\tilde{\rho}} = 0$.

The second variation of the Gibbs free energy, $\delta^2 G$, is also more easily derived by using the potential. From the first variation $\delta G = G_{\tilde{\rho}}\delta\tilde{\rho} + \delta_\phi G$, where $\delta_\phi G$ indicates the volume fraction variation of the potential at constant T, P, and $\tilde{\rho}$

$$\delta_\phi G = \left.\frac{\partial G(\tilde{\rho},\phi+t\delta\phi)}{\partial t}\right|_{t=0,\tilde{\rho},T,P} \tag{21}$$

follows the second variation

$$\delta^2 G = [\delta_\phi{}^2 G + 2\delta_\phi G_{\tilde{\rho}}(\delta\tilde{\rho}) + G_{\tilde{\rho}\tilde{\rho}}(\delta\tilde{\rho})^2] + G_{\tilde{\rho}}\delta^2\tilde{\rho} \tag{22}$$

The last term of relation 22 is zero on the free energy surface, $G_{\tilde{\rho}} = 0$, but the first is also restricted by $\delta G_{\tilde{\rho}} = G_{\tilde{\rho}\tilde{\rho}}\delta\tilde{\rho} + \delta_\phi G_{\tilde{\rho}} = 0$ or $\delta\tilde{\rho} = -\delta_\phi G_{\tilde{\rho}}/G_{\tilde{\rho}\tilde{\rho}}$. With these substitutions eq 22 becomes

$$\begin{aligned} \delta^2 G &= \delta_\phi{}^2 G - \frac{(\delta_\phi G_{\tilde{\rho}})^2}{G_{\tilde{\rho}\tilde{\rho}}} \\ &= \delta_\phi{}^2 G - G_{\tilde{\rho}\tilde{\rho}}(\delta\tilde{\rho})^2 \end{aligned} \tag{23}$$

For an incompressible fluid this equation reduces to the Flory–Huggins formulation $\delta^2 G = \delta_\phi{}^2 G$ since $G_{\tilde{\rho}\tilde{\rho}}{}^{-1} \sim \kappa = 0$[45] where κ is the isothermal compressibility $-1/V\ \partial V/\partial P|_T$.

Unless vectors $\delta\phi_i$ and $\epsilon_{(ii)}^*$ are nearly perpendicular

$$\delta_\phi G_{\tilde{\rho}} \approx \delta_\phi H_{\tilde{\rho}} \approx -\sum_{i=1}^{r} \epsilon_{(ii)}^*(\delta\phi_i) \tag{24}$$

since vaporization energy terms ($\epsilon_{(ii)}^*$) are 2–3 orders of magnitude larger than interaction energy ($\Delta\epsilon_{(ij)}^*$) and excess entropy ($1/r_i$) terms. As temperature increases, so generally does $G_{\tilde{\rho}\tilde{\rho}}{}^{-1}$ and, therefore, the compressible term driving phase separation on heating (LCST behavior). The combinatorial entropy $\delta_\phi{}^2 S = \delta^2 S^{(c)}$ is still important for describing USCT behavior. Generally, modified Flory–Huggins and lattice fluid theories describe the same phase stability–temperature behavior; for example, USCT followed by LCST behavior for the latter is depicted in diagram d of Figure 2. Similarly, if combinatorial entropy is negligible and the compressibilities of component polymers are similar, the addition of any number of components to an immiscible binary (i–j) does not solubilize it

$$\min \delta^2 G \le \delta^2 G(\delta\phi_i{=}{-}\delta\phi_j, \delta\phi_{k\neq i,j}{=}0) \approx \left[kT(\eta_i + \eta_j) - 2\tilde{\rho}\Delta\epsilon_{(ij)}^* - \frac{(\epsilon_{(ii)}^* - \epsilon_{(jj)}^*)^2}{G_{\tilde{\rho}\tilde{\rho}}} \right](\delta\phi_i)^2 \tag{25}$$

where $\eta_i = 1/\phi_i r_i$. Multicomponent cloud-point temperatures associated with LCST behavior bounded by the smallest binary values are a corollary of this. Binary spinodal temperatures diverge for very large molecular weights when $\epsilon_{(ii)}^* - \epsilon_{(jj)}^* \approx 0$ corresponding to $B_{(ij)}{}^s \approx 0$ of the modified Flory–Huggins theory. The former is bounded by the liquid–gas spinodal temperature, $1/\kappa \to 0$; a sharp peak forms instead of a hyperbolic asymptote (Figure 3) of *mer* content or polymer composition. If the spinodal divergence is located near a miscibility boundary, compressibility terms may be small enough to allow a UCST to merge with an LCST there. Although this may not be observable because the spinodal temperature is below the glass transition, it makes multicomponent UCST behavior more likely. Crude $T_i^* = \epsilon_{ii}^*/k$ *mer* estimates[40a] predict that a spinodal divergence lies within the SMA/SAN miscibility diagram but closer to the opposite miscibility boundary than cloud-point observations or excess entropy parameters, $B_{(ij)}{}^s$, in Table III would indicate. However, these estimates (T^*_{SAN}, $T^*_{SMA} > T^*_{PMA}$, where PMA = PMMA or PEMA) also indicate, as do cloud-point observations and excess entropy parameters, that there are no such divergences within the miscibility windows of SAN/polymethacrylate or SMA/polymethacrylate blends.

If combinatorial entropy is negligible and $(\tilde{\rho}G_{\tilde{\rho}\tilde{\rho}})^{-1}$ can be approximated by the same linear function of temperature over the interval from T_g to the temperature where chemical degradation occurs for each binary, the modified Flory–Huggins theory can accurately describe the second variation of Gibbs free energy, $\delta^2 G$, as well as enthalpy

$$\begin{aligned} \delta^2 H &= [\delta_\phi{}^2 H + 2\delta_\phi H_{\tilde{\rho}}(\delta\tilde{\rho}) + H_{\tilde{\rho}\tilde{\rho}}(\delta\tilde{\rho})^2]_{\delta G_{\tilde{\rho}}=0} + H_{\tilde{\rho}}\delta^2\tilde{\rho} \\ &\approx \delta_\phi{}^2 H + 2TS_{\tilde{\rho}\tilde{\rho}}{}^{(e)}(\delta\tilde{\rho})^2 + H_{\tilde{\rho}}\delta^2\tilde{\rho} \end{aligned} \tag{26}$$

for multicomponent mixtures with the same *mer* units when excess entropy parameters are approximately related "regularly"

$$(-B_{mn}{}^s)^{1/2} \approx (-B_{mq}{}^s)^{1/2} + (-B_{nq}{}^s)^{1/2} \tag{27}$$

An accurate $\delta^2 H$ value is necessary to calculate ternary spinodal temperatures far different from the binaries, a common trait of a large LCST drop, or the appearance of a UCST. For an incompressible fluid ($\delta\tilde{\rho} = \delta^2\tilde{\rho} = 0$) the formal Flory–Huggins relation is retrieved. Because nearly every $B_{mn}{}^s$ value in Table III is positive, relation 27 is never satisfied. Furthermore, $-\delta^2 S^{(e)}$ and $-(\delta_\phi G_{\tilde{\rho}})^2$ have opposite curvature as a function of *mer* content over the homopolymer/copolymer miscibility windows; the first is convex and the second concave. Such considerations are especially important when $\delta_\phi{}^2 H$ of eq 26 is driven near zero by asymmetry of binary interactions to produce interesting multicomponent phase behavior.

Selection of Ternary Blends

The purpose of the experimental part of this work has been to examine some ternary blends to see if examples can be found of the ternary instability discussed above in the form of either a large decrease in the ternary LCST or the appearance of a ternary UCST. As mentioned before, combinations of a polymethacrylate with SAN and SMA copolymers offer unique opportunities for exploring this possibility since the polymer–polymer binary interaction energies, $B_{(ij)}$, can be manipulated by varying the AN and MA contents of the copolymers. An exhaustive search of all possibilities is impractical so we restricted the study to a few ternaries that might offer interesting

Table V
Ternary Blends Studied Here

blend syst	MA content of SMA, wt %	AN content of SAN, wt %	third polymer	blend preparn method
1	14	9.5	PMMA	melt
2	25	25	PMMA	solution
3	25	30	PMMA	melt
4	14	9.5	PEMA	melt
5	17	11.5	PEMA	melt
6	25	25	PEMA	solution
7	25	20.5	MAN12	melt

behavior. In this section we review the rationale for selecting the systems we used (see Table V). These choices are summarized graphically in Figure 4.

Figure 4a shows the approximate regions of copolymer composition where each binary pair in the system SMA/SAN/PMMA forms miscible blends while Figure 4b replaces PMMA by PEMA. In Figure 4c, the third material is a copolymer of methyl methacrylate and acrylonitrile. Within the shaded common region all three binary pairs are miscible. More specifically, the dotted lines define boundaries where the polymer–polymer binary interaction energy density, $B_{(ij)}$, is zero at T_g. These correspond to the miscibility–immiscibility boundaries except for a small widening from either the combinatorial entropy contribution when molecular weights are finite or the observed cloud-point tail near the upper AN boundary of SAN/PMMA miscibility.[22] The upper boundaries of MA content for SMA/polymethacrylate miscibility are experimentally bounded by 33 and 47 wt % MA.[38] The $B_{(ij)}$ are related to the monomer unit pair interactions, B_{mn}, and to copolymer composition by appropriate versions of eq 8 for the various homopolymer/copolymer or copolymer/copolymer mixtures.[39] The boundaries shown in Figure 4 were computed by using the B_{mn} values in Table III. The shaded regions are where the polymer–polymer interaction energies for all three binary pairs are negative. As one of the miscibility boundaries is approached, the cloud point of the corresponding binary converges toward T_g. Near the upper SMA/SAN boundary, the temperature-dependent B_{mn}s in Table III result in a calculated divergence of the spinodal temperature. No LCST behavior has been experimentally found in this region, and from the results available it is estimated that the cloud-point surface must have a slope greater than 150 °C/wt % MA content.

From the analysis described above, we know that when all three binary polymer–polymer intactions are comparable, $\delta^2 H$ is similar for binary and ternary. This is the situation in the middle of the shaded regions. Systems 2 and 6 (see Figure 4 and Table VI) are of this type and cloud points would be expected to vary smoothly over these ternary regions. Ternary instabilities are driven by asymmetry in the polymer–polymer interaction energies for the binaries, and this would be more likely to exist near one of the miscibility boundaries or a corner where two intersect. The other systems shown (see Figure 4 and Table VI) were selected, within the constraints of available copolymer compositions, to probe these areas for examples of ternary instability.

Spinodal temperatures were calculated from eq 5 by using the modified Flory–Huggins theory with temperature-dependent B_{mn} (Table III), molar volume $V = 10^5$ cm^3/mol and *mer* volume fractions based on van der Waals volumes[54] inserted into expression 8 for each binary. Larger molar volumes depress the predicted LCST and enhance the UCST but essentially do not change the character of the predictions. Three of these predictions,

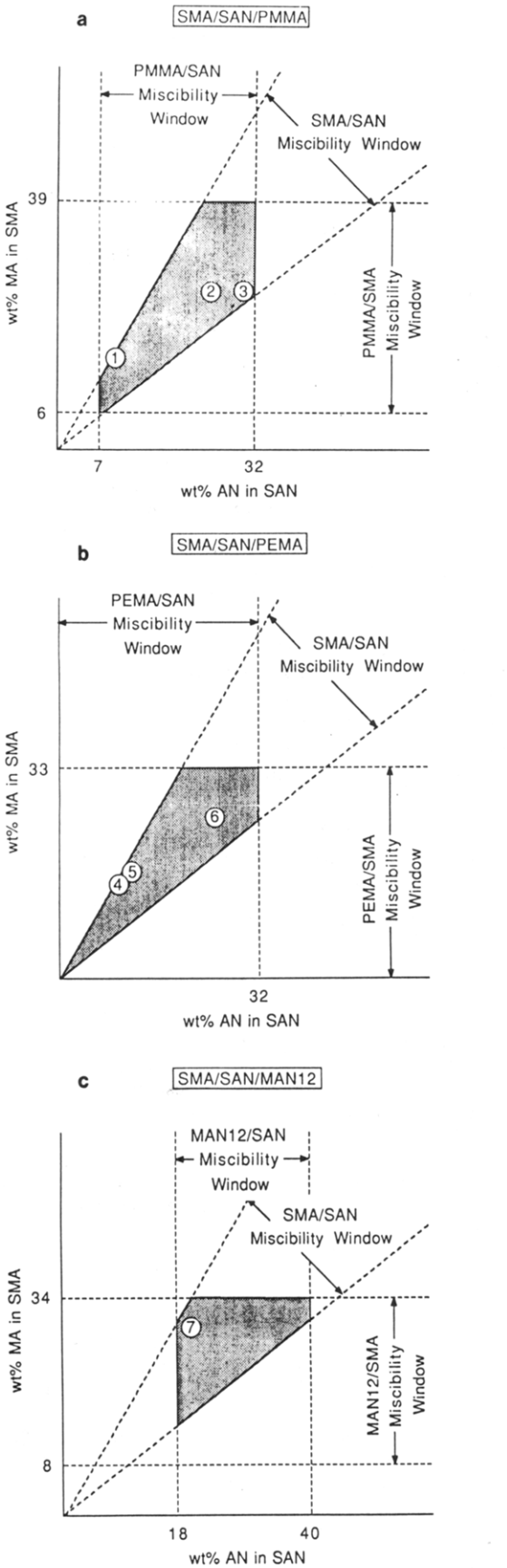

Figure 4. Diagrams defining the regions of SMA and SAN copolymer compositions (between dashed line pairs) where each binary interacts exothermically and is miscible in the high molecular weight limit ($1/V = 0$). The third polymer is PMMA in (a), PEMA in (b), and MAN copolymer is (c). Within the shaded regions, where all binary pairs are miscible, the circled numbers represent the placement of the ternary systems listed in Table V.

Table VI
Polymers Used in This Study

polymer[a]	mol wt info	T_g, °C	source
SMA14	M_n = 90 000 M_w = 180 000	128	Arco Chemical Co. (Dylark 332)
SMA17	nd[d]	132	Arco Chemical Co.
SMA25[c]	η = 4.73[b]	149	Monsanto Co.
SAN9.5	nd	103	Asahi Chemical
SAN11.5	nd	104	Asahi Chemical
SAN20.5	M_w = 193 800	107	Dow Chemical Co.
SAN25	M_n = 75 800 M_w = 160 000	109	Dow Chemical Co.
SAN30	M_n = 81 000 M_w = 168 000	109	Dow Chemical Co.
MAN12	η = 3.40[b]	nd	Asahi Chemical
poly(methyl methacrylate)	M_n = 52 900 M_w = 130 000	108	Rohm & Haas V(811)100
poly(ethyl methacrylate)	M_w = 438 000	71	Du Pont, Elvacite 2042

[a] SMA denotes styrene/maleic anhydride copolymer, SAN styrene/acrylonitrile copolymer, and MAN methyl methacrylate/acrylonitrile copolymer. The number following each acronym denotes weight percent of second monomer. [b] Viscosity of a 10 wt % solution in methyl ethyl ketone at 25 °C in mPa·s. [c] SMA25 contains 25 wt % maleic anhydride and a small amount of a third monomer in addition to styrene. [d] nd = not determined.

shown in Figure 12, proved to be qualitatively wrong. For the other systems the spinodal temperature associated with the LCST varied smoothly as did the experimental cloud point. The lower binary cloud-point temperature propagates through much of the ternary, but combinatorial entropy is an important factor.

Materials and Experimental Procedures

Table VI lists the various polymers used in this work and their sources. Seven ternary blends were prepared from various combinations of these materials as described in Table V. For each ternary, the three corresponding binary blends are miscible as described elsewhere.[22,38,40] Two blend preparation techniques were used in this work: solution casting from methyl ethyl ketone with final drying in a vacuum oven for 2 days at 20 °C above T_g and melt mixing in a Brabender or in a CSI Mini-Max molder. All binary blends were made by solvent casting except for SMA14 and PMMA, which were made by melting mixing.[38] Similarly, all ternary compositions except those of systems 2 and 6 were melt mixed. The explanation for this is given in the next section.

When applicable, miscibility was judged by the T_g behavior of the mixtures using a Perkin-Elmer DSC-2 or DSC-7 at a heating rate of 20 °C/min. Glass transitions reported are from second heats and were calculated by the onset method. In several cases, miscibility was confirmed by the occurrence of phase separation on heating, indicative of LCST behavior. In most of these cases, a visual cloud point was measured at a heating rate of 2 °C/min over a restricted temperature interval initially defined by a scan at 10 °C/min.[55] For SMA/SAN binary blends, when both components have similar refractive indices,[40a] the phase-separation temperature was estimated as the average of adjacent annealing temperatures (10 °C increments) that produced one or two glass transitions.[56]

Densities of selected samples were measured at 30 °C by using a density gradient column based on calcium nitrate. Specific heats were measured at 5 °C/min with the DSC-7 using a sapphire standard.[57] Since all excess volumes and heat capacities were found to be zero within experimental error, these results will not be discussed in further detail.

Experimental Results

Considerable care must be exercised in the preparation of some polymer blends if one wishes to be sure that the state of mixing achieved represents the equilibrium one. Solution-casting techniques can lead to phase-separated mixtures from miscible pairs because a closed-loop immiscibility region is traversed on solvent evaporation.[36,58] On the other hand, we have recently shown that some solution preparation methods can trap an immiscible pair into a homogenous, but nonequilibrium, state.[59] Melt mixing above an LCST (or below a UCST) phase boundary can lead to the conclusion that a pair is not miscible, when at another temperature they may be fully so. The converse situation of achieving a nonequilibrium homogenous state by melt mixing seems much less likely.[60] Being aware of these possibilities, we have been very diligent to ensure that the observations reported here do reflect, in our opinion, equilibrium results.

All of the binary pairs considered here gave equilibrium, homogenous blends by solvent casting from MEK except for one. As described previously,[38] PMMA forms miscible blends with SMA14, but solvent casting may not give a homogenous mixture. In the present case, this pair was melt blended.

Ternary systems 2 and 6 were solution cast because any asymmetry of solvent–polymer interactions was thought to be minor compared to the combinatorial entropy of adding the liquid. All other ternary systems were melt blended because the addition of solvent could easily exacerbate the local ternary instability sought. Melt temperatures of 170–180 °C seemed sufficient for good mixing. Inhomogenous samples remained so after mixing at 200 °C. Where a large decrease in the cloud-point temperature (relative to binary values) was recorded within the ternary region, samples were annealed in 40 °C intervals above this temperature for 10 min each. If kinetics were not limiting, the absence of any indication of phase homogenization would serve as a crude verification that UCST phenomena are not observed at higher temperatures than the LCST for any of these systems.

Next, we describe the observations made for each system. For ease of presentation, the glass transitions and cloud points found for each system are shown on adjacent triangular diagrams with the values located according to composition. Some blends did not phase separate prior to severe decomposition (usually 300 °C or above), and these cases are noted by the symbol D. Cloud points are, of course, meaningless for pure components, and in other cases they were not measured. Both cases are denoted by an asterisk.

Figure 5 shows the results for system 1. Each blend has a single T_g, but owing to the closeness of the values for PMMA and SAN, this is not adequate proof of a single phase. All blends were clear following melt blending (contrary to results obtained by solvent casting) but phase separated on heating as shown in Figure 5 except for the SMA/SAN binary that remained transparent and had one T_g to decomposition. This is, of course, proof of miscibility for the entire ternary composition spectrum. It is interesting to note that the cloud points of the ternary compositions are always lower than those of the binaries falling as low as 211 °C at one composition.

Results for system 2 are shown in Figure 6. Again, each composition shows a single T_g, and the blends were transparent following melt mixing. Only the PMMA/SAN binary exhibits phase separation on heating while the other two remained clear to decomposition. Most ternary compositions did phase separate on heating but at progressively higher temperatures as the composition moved away from the PMMA/SAN binary leg. This simple behavior is what one might expect of a ternary well within the miscibility regions for each binary (see Figure 4).

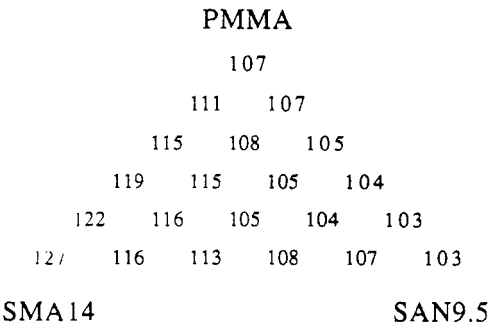

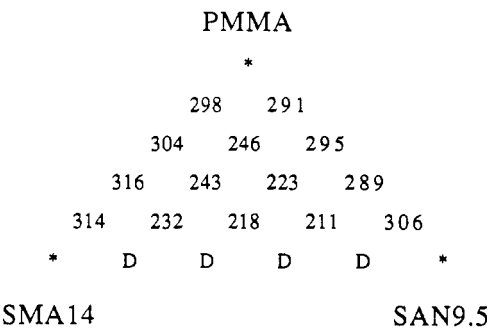

Figure 5. System 1: T_g (above) and cloud-point temperature (below) all in degrees Celsius shown on a triangular diagram to indicate ternary compositions. All compositions are equally spaced on this and subsequent diagrams. An asterisk is used to indicate that the value does not exist (e.g., cloud point for pure component) or was not measured. System 1 is defined in Table V. D indicates that degradation occurs before cloud-point temperature is reached.

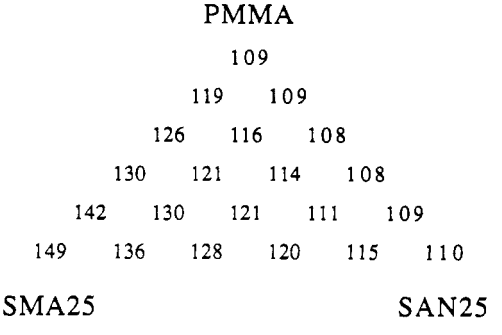

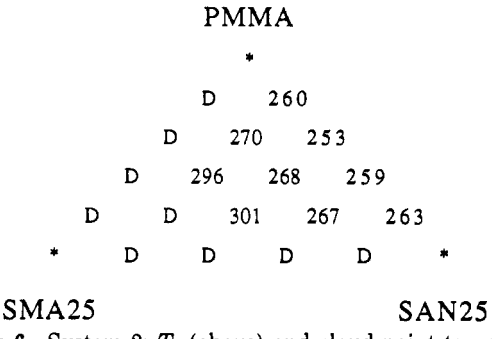

Figure 6. System 2: T_g (above) and cloud-point temperature (below) all in degrees Celsius. See Figure 5 for notation.

System 3 has three ternary compositions, which are not transparent when melt mixed at 180 °C and have two glass transitions (Figure 7). The cloud points for the PMMA/SAN binary are just over 200 °C, whereas the other two binaries do not phase separate prior to decomposition. Evidently, the ternary cloud-point surface dips below the 180 °C mixing temperature near the PMMA/SAN binary leg (the cause for two glass transitions) and then climbs above this level toward the SMA apex. Thus, this system seems to demonstrate that the ternary LCST decreases toward T_g in the right-hand limit of the shaded region of Figure 4a. On the basis of these observations, we cannot say that the coexistence surface drops below the glass transition surface, but with increasing AN content in the SAN, this is likely (replace SAN30 by SAN34, for example). Since melt mixing at lower temperatures is not practical and solvent casting may lead to nonequilibrium mixed or unmixed states, we did not pursue this question further.

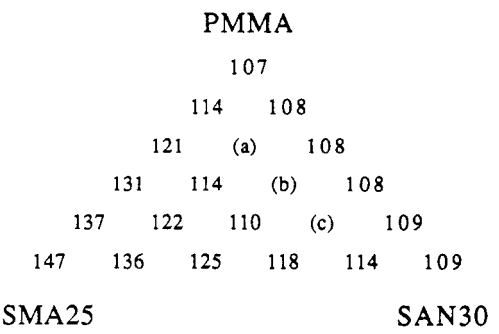

	(a)	(b)	(c)
Two T_g's	110	104	105
Observed:	140	140	141

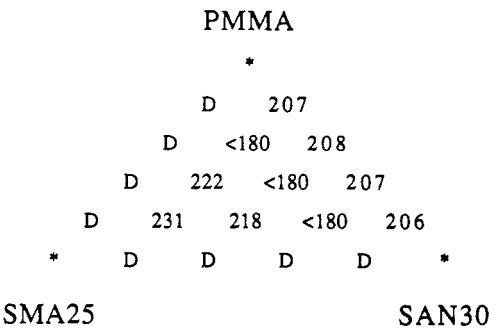

Figure 7. System 3: T_g (above) and cloud-point temperature (below) in degrees Celsius. Three ternary compositions had two glass transitions as shown; D indicates degradation of polymers before cloud point; <180 indicates that cloud-point temperature is below a melt mixing temperature of 180 °C.

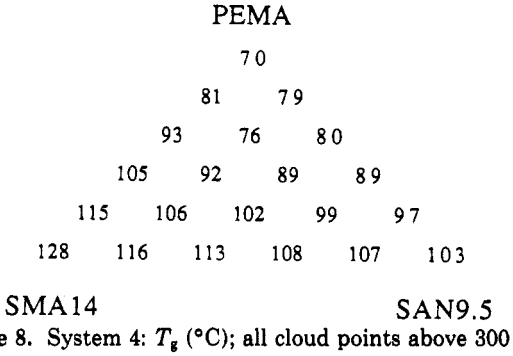

Figure 8. System 4: T_g (°C); all cloud points above 300 °C.

All of the ternary blends based on PEMA as the third component, systems 4–6, exhibited a single T_g everywhere as seen in Figures 8–10. Because of the large differences in the glass transitions of the three components, this fact is good evidence for a single phase. All binary and ternary compositions for systems 4 and 5 remained transparent on heating to 300 °C, beyond which degradation was a significant factor. However, for system 6 the PEMA/SAN and PEMA/SMA binaries show phase separation at measurable temperatures as seen in Figure 10, whereas the

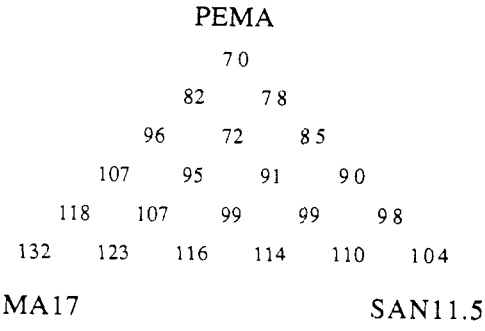

Figure 9. System 5: T_g (°C); all cloud points above 300 °C.

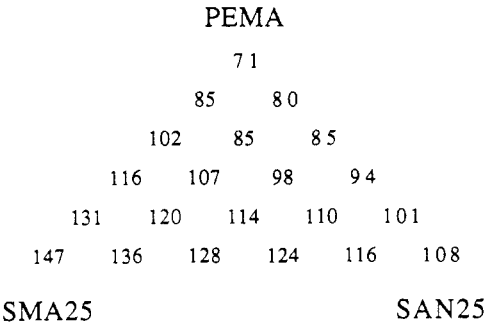

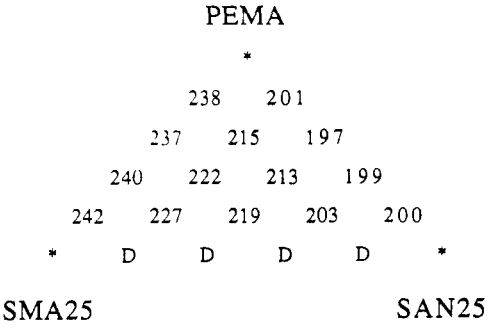

Figure 10. System 6: T_g (above) and cloud point temperature (below) in °C.

SAN/SMA binary decomposes first. For this system, the cloud-point surface in the ternary region is always intermediate to values shown on the PEMA/SAN and PEMA/SMA binary legs; however, the surface evidently must rise steeply as the SMA/SAN binary leg is approached since it presumably has a very high cloud-point curve. All in all, there is no real evidence that the ternaries involving PEMA are more prone to phase separation than are the respective binaries.

Recently, we have studied[61] blends involving methyl methacrylate/acrylonitrile copolymers, MAN, and found them to be interesting candidates for inclusion in the present investigation. Figure 11 shows sparse cloud-point results for ternary blends involving one of these MAN materials, system 7. The blends were melt mixed at 180 °C. As shown, the MAN/SAN and MAN/SMA binaries phase separate on heating only at very high temperatures while SMA/SAN binary blends decompose first. All ternary compositions tested had very significantly lower cloud points, and one composition was cloudy as prepared, indicating possibly that the cloud point is <180 °C. Unfortunately, glass transition behavior would not be very informative about the state of mixing, owing to the similarity of the SAN and MAN T_g values. This system seems to be an example of ternary instability and deserves further study.

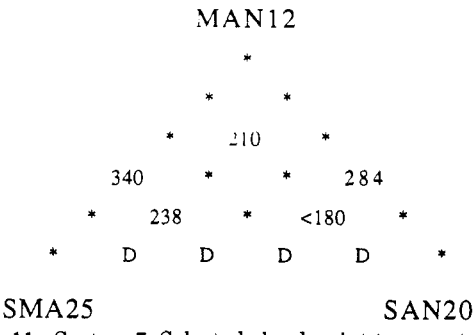

Figure 11. System 7: Selected cloud-point temperatures (°C); T_g not determined; D indicates degradation of polymers before cloud point; <180 indicates that cloud point is below a melt mixing temperature of 180 °C.

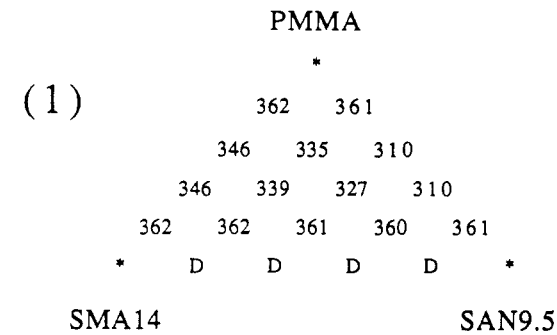

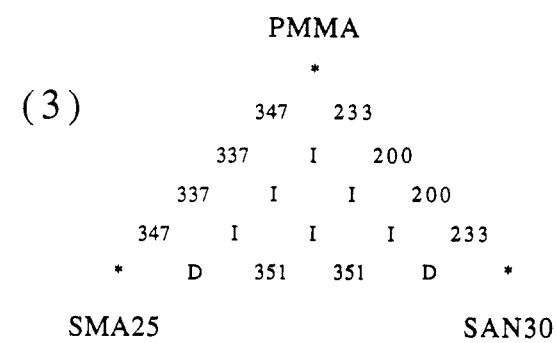

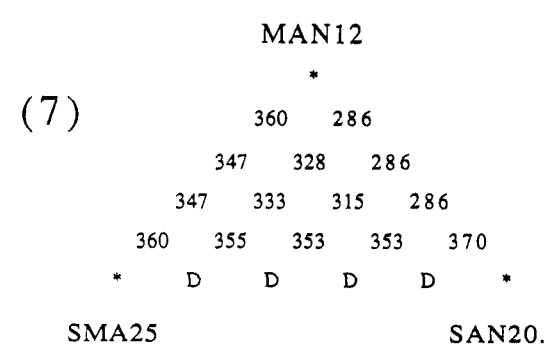

Figure 12. Predicted spinodal temperatures (°C) associated with LCST calculated by using Flory–Huggins *mer* interaction parameters, $B_{ij}^h - TB_{ij}^s$, of Table III and molar volume = 10^5 cm^3/mol; D indicates temperatures above 300 °C or that polymer degradation is likely to occur before phase separation; I indicates that blend is predicted to be immiscible within the temperature range from T_g up to degradation.

The miscalculations presented in Figure 12 illustrate several points. First, the predicted spinodal temperatures of the MAN12 binaries of system 7 are quite close to the experimental cloud-point temperatures (Figure 11), closer in fact than some of the correlated binaries. For example, correlation is poor for the binary blend SMA14/PMMA

because the cloud point decreases sharply as MA content decreases toward the miscibility boundary.[38] Second, uniform cloud-point variation far above ternary UCST (not shown) is calculated for blends 1 and 7 when in fact a large decrease of cloud point to the temperature range of predicted UCST was observed within the ternary region. The incorrect weighting of δ^2H and δ^2S at the spinodal temperature could be largely affected by the placement of the SMA/SAN binaries near the calculated spinodal divergence (Figure 3). Finally, for system 3 the ternary cloud point is predicted to fall below T_g, rendering most compositions immiscible at all temperatures while experimentally only a small decrease below binary values is observed. Perhaps the discrepancy stems from the poorly established upper MA miscibility boundary of the binary SMA/PMMA and the opposite curvature of $-\delta^2S^{(e)}$ and $-(\delta_\phi G_{\tilde{p}})^2$ for this binary as a function of *mer* content.

Conclusion

Cloud points of various ternary blends consisting of three miscible binary pairs have been compared. Both a large drop and smooth variation of cloud-point temperatures between binary values were observed. The former occurred when binary pairs were located near the corner of the three intersecting miscibility windows.

Although all binaries are miscible and have exothermic interactions, immiscibility of multicomponent polymer or solvent–polymer mixtures can result from an asymmetry of binary interactions, the $\Delta\chi$ effect.[36] In addition to the large drop in cloud point that has been observed, the appearance of a ternary UCST can result from this effect. Although the combinatorial entropy that is responsible for the latter is much smaller than the enthalpy at large molecular weights, similar second variations can be obtained (Table IV). Note that between every two points on a phase diagram that are in equilibrium with each other there must be at least two spinodal points defined by a minimum second variation of Gibbs's free energy of zero. Alternatively, asymmetric interactions may cause a binary UCST to increase to observable temperatures. The spinodal condition for this and a mixture of a homopolymer and copolymer with distribution in *mer* content are equivalent.[48] With the appropriate choice of molecular weight and *mer* content (and distribution), there is reason to believe that UCST behavior can occur.

Interesting spinodal calculations (Figure 12), which included UCST predictions, were uniformly inaccurate. Although the binary spinodal temperature root of $\delta^2H = T\delta^2S$ may be accurately correlated over the various miscibility windows, the size dependence as a function of *mer* content may be incorrect. This can lead to (1) artificial spinodal temperature divergences and (2) false multicomponent predictions. None of this proves that the modified Flory–Huggins approach[42] is necessarily inaccurate for the class of ternary blends considered here.

Acknowledgment. This research was sponsored in part by the National Science Foundation and by the Air Force Office for Scientific Research.

References and Notes

(1) Kwei, T. K.; Frisch, H. L.; Radigan, W.; Vogel, S. *Macromolecules* **1977**, *10*, 157.
(2) Wang, Y.-Y.; Chen, S.-A. *Polym. Eng. Sci.* **1981**, *21*, 47.
(3) Rigby, D.; Lin, J. L.; Roe, R. J. *Macromolecules* **1985**, *18*, 2269.
(4) Shah, V.; Keitz, J. D.; Paul, D. R.; Barlow, J. W. *J. Appl. Polym. Sci.* **1986**, *32*, 3863.
(5) Equizabal, J. I.; Irvin, J. J.; Cotazar, M.; Guzman, G. M. *J. Appl. Polym. Sci.* **1986**, *32*, 5945.
(6) Goh, S. H.; Siow, K. S.; Yap, K. S. *Thermochim. Acta* **1986**, *105*, 191.
(7) Goh, S. H.; Siow, K. S. *Thermochim. Acta* **1986**, *102*, 281.
(8) Christiansen, W. H.; Paul, D. R.; Barlow, J. W. *J. Appl. Polym. Sci.* **1987**, *34*, 537.
(9) Landry, C. J. T.; Yang, H.; Machell, J. S., to be submitted for publication.
(10) Min, K. E.; Chiou, J. S.; Barlow, J. W.; Paul, D. R. *Polymer* **1987**, *28*, 1721.
(11) Factor, A.; Orlando, C. M. *J. Polym. Sci., Polym. Chem. Ed.* **1980**, *18*, 579.
(12) Paul, D. R., unpublished results.
(13) (a) Fischer, E. W.; Hellman, G. P.; Spiess, H. W.; Horth, F. J.; Ecarius, U.; Wehrle, M. *Makromol. Chem., Suppl.* **1985**, *12*, 189. (b) Freitag, D.; Grigo, U.; Muller, P. R.; Nouvertne, W. In *Encyclopedia of Polymer Science and Engineering*, 2nd ed.; Mark, H. F., Bikales, N. M., Overberger, C. G., Menges, G., Eds.; John Wiley: New York, 1988; Vol. 11, p 655.
(14) Fernandes, A. C.; Barlow, J. W.; Paul, D. R. *Polymer* **1986**, *27*, 1799.
(15) (a) Wahrmund, D. C.; Barlow, J. W.; Paul, D. R. *J. Appl. Polym. Sci.* **1978**, *22*, 2155. (b) Nassar, T. R.; Barlow, J. W.; Paul, D. R. *J. Appl. Polym. Sci.* **1979**, *23*, 85. (c) Cruz, C. A.; Barlow, J. W.; Paul, D. R. *J. Appl. Polym. Sci.* **1979**, *24*, 2101, 2399; **1980**, *25*, 1549. (d) Smith, W. A.; Barlow, J. W.; Paul, D. R. *J. Appl. Polym. Sci.* **1981**, *26*, 4233. (e) Barnum, R. S.; Barlow, J. W.; Paul, D. R. *J. Appl. Polym. Sci.* **1982**, *27*, 4065.
(16) Woo, E. M.; Barlow, J. W.; Paul, D. R. *J. Appl. Polym. Sci.* **1983**, *28*, 1347; **1986**, *32*, 3889.
(17) Woo, E. M.; Barlow, J. W.; Paul, D. R. *J. Appl. Polym. Sci.* **1985**, *30*, 4243.
(18) (a) Ziska, J. J.; Barlow, J. W.; Paul, D. R. *Polymer* **1981**, *22*, 918. (b) Woo, E. M.; Barlow, J. W.; Paul, D. R. *Polymer* **1985**, *26*, 763.
(19) (a) Fernandes, A. C.; Barlow, J. W.; Paul, D. R. *J. Appl. Polym. Sci.* **1986**, *32*, 5357. (b) Chiu, S.-C.; Smith, T. G. *J. Appl. Polym. Sci.* **1984**, *29*, 1797.
(20) Fowler, M. E.; Paul, D. R.; Cohen, L. A.; Freed, W. T. *J. Appl. Polym. Sci.* **1989**, *37*, 513.
(21) Kim, J. H.; Barlow, J. W.; Paul, D. R. *J. Polym. Sci., Part B: Polym. Phys.*, in press.
(22) (a) Fowler, M. E.; Barlow, J. W.; Paul, D. R. *Polymer* **1987**, *28*, 1177. (b) Stein, V. D. J.; Jung, R. H.; Illers, K. H.; Hendus, H. *Angew. Makromol. Chem.* **1974**, *36*, 89. (c) Seuss, M.; Kressler, J.; Kammer, H. W. *Polymer* **1987**, *28*, 957. (d) Cowie, J. M. G.; Lath, D. *Makromol. Chem., Macromol. Symp.* **1988**, *16*, 103; *Polym. Commun.* **1987**, *28*, 300.
(23) Woo, E. M. Barlow, J. W.; Paul, D. R. *J. Polym. Sci., Polym. Symp.* **1984**, *72*, 137.
(24) Goh, S. H.; Paul, D. R.; Barlow, J. W. *Polym. Eng. Sci.* **1982**, *22*, 34.
(25) Kim, J. H.; Barlow, J. W.; Paul, D. R. *Polym. Eng. Sci.* **1989**, *29*, 581.
(26) Chiou, J. S.; Paul, D. R. *J. Appl. Polym. Sci.*, in press.
(27) (a) Martuscelli, E.; Demma, G. B. In *Polymer Blends: Processing Morphology and Properties*; Martuscelli, E., Palumbo, R., Kryszewski, M., Eds.; Plenum Press: New York, 1980. (b) Cortazar, M. M.; Calahorra, M. E.; Guzman, G. M. *Eur. Polym. J.* **1982**, *18*, 165. (c) Martuscelli, E.; Canetti, M.; Vicini, L.; Serves, A. *Polym. Commun.* **1983**, *24*, 331. (d) Calahorra, E.; Cortazar, M.; Guzman, G. M. *Polymer* **1982**, *23*, 1322. (e) Fernandez-Berridi, M. J.; Guzman, G. M.; Irvin, J. J.; Elonza, J. M. *Polymer* **1983**, *24*, 217. (f) Martuscelli, E.; Demma, G.; Rossi, E.; Segre, A. L. *Polym. Commun.* **1983**, *24*, 266. (g) Calahora, E.; Cortazar, M.; Guzman, G. M. *Polym. Commun.* **1983**, *24*, 211. (h) Martuscelli, E.; Pracella, M.; Wang, P. Y. *Polymer* **1984**, *25*, 1097. (i) Li, X.; Hsu, S. L. *J. Polym. Sci., Polym. Phys. Ed.* **1984**, *22*, 1331. (i) Liberman, S. A.; de Gomes, A. S.; Macchi, E. M. *J. Polym. Sci., Polym. Chem. Ed.* **1984**, *22*, 2809. (j) Romana Ras, G.; Castiglioni, C.; Gussoni, M.; Zerbi, G.; Martuscelli, E. *Polymer* **1985**, *26*, 811.
(28) Robeson, L. M.; Hale, W. F.; Merriam, C. N. *Macromolecules* **1981**, *14*, 1644.
(29) Walsh, D. J.; Singh, V. B. *Makromol. Chem.* **1984**, *185*, 1979.
(30) Paul, D. R., unpublished results.
(31) Keskkula, H. K.; Paul, D. R. *J. Appl. Polym. Sci.* **1986**, *31*, 1189.
(32) Fernandes, A. C.; Barlow, J. W.; Paul, D. R. *J. Appl. Polym. Sci.* **1986**, *32*, 6073.
(33) Nandi, A. K.; Mandal, B. M.; Bhattacharyya, S. N. *Macromolecules* **1985**, *18*, 1454.
(34) El-Hibri, M. J.; Munk, P. *Polym. Prepr. (Am. Chem. Soc., Div. Polym. Chem.)* **1987**, *28*, 262.
(35) Martuscelli, E.; Silvestre, C.; Gismondi, C. *Makromol Chem.* **1985**, *186*, 2161.

(36) (a) Su, C. S.; Patterson, D. *Macromolecules* **1977**, *10*, 709. (b) Robard, A.; Patterson, D. *Macromolecules* **1977**, *10*, 1021. (c) Bhattacharyya, C.; Maiti, N.; Mandal, B. M.; Bhattacharyya, S. N. *Macromolecules* **1989**, *22*, 487.
(37) Kehlen, H.; Raetzsch, M. T.; Bergmann, J. *J. Macromol. Sci., Chem.* **1987**, *A24*, 1.
(38) Brannock, G. R.; Barlow, J. W.; Paul, D. R. submitted for publication in *J. Polym. Sci.*
(39) (a) Paul, D. R.; Barlow, J. W.; Keskkula, H. In *Encyclopedia of Polymer Science and Engineering*, 2nd ed.; Mark, H. F., Bikales, N. M., Overberger, C. G., Menges, G., Eds.; John Wiley: New York, 1988; Vol. 12, p 399. (b) Nishimoto, M.; Keskkula, H.; Paul, D. R. *Polymer* **1989**, *30*, 1279.
(40) (a) Kim, J. H.; Barlow, J. W.; Paul, D. R. *J. Polym. Sci., Part B: Polym. Phys.* **1989**, *27*, 223. (b) Kressler, J.; Kammer, H. W.; Schmidt-Naake, G.; Herzog, K. *Polymer* **1988**, *29*, 686. (c) Aoki, Y. *Macromolecules* **1988**, *21*, 1277. (d) Hall, W. J.; Kruse, R. L.; Mendelson, R. A.; Trementozze, Q. A. *Prepr. Am. Chem. Soc. Div. Org. Coatings Plast. Chem.* **1982**, *47*, 298; *Am. Chem. Soc. Symp. Ser.* **1983**, *229*, 49.
(41) (a) Paul, D. R.; Barlow, J. W. *Polymer* **1984**, *25*, 487. (b) Kambour, R. P.; Bendler, J. T.; Bopp, R. C. *Macromolecules* **1983**, *16*, 753. (c) ten Brinke, G.; Karasz, F. E.; MacKnight, W. J. *Macromolecules* **1983**, *16*, 1827.
(42) (a) Flory, P. J. *Principles of Polymer Chemistry*; Cornell University Press: Ithaca, NY, 1955; p 523. (b) Barnum, R. S.; Goh, S. H.; Barlow, J. W.; Paul, D. R. *J. Polym. Sci., Polym. Lett. Ed.* **1985**, *23*, 395.
(43) Brannock, G. R. Ph.D. Thesis, Department of Chemical Engineering, University of Texas, Austin, TX, 1990; Chapter 5.
(44) Sanchez, I. C.; Lacombe, R. H. *Macromolecules* **1978**, *6*, 1145.
(45) Sanchez, I. C.; Balazs, A. C. *Macromolecules* **1989**, *22*, 2325.
(46) (a) Tisza, L. *Generalized Thermodynamics*; MIT Press: Cambridge, MA, 1966; pp 147, 187. (b) Ferrar, W. L. *Algebra*; Clarendon Press: Oxford, 1941; p 135.
(47) (a) Schmitt, B. J. *Angew. Chem., Int. Ed. Engl.* **1979**, *18*, 273. (b) Koningsveld, R.; Kleintjens, L. A. In *Polymer Blends and Mixtures*, Walsh, D. J., Higgins, J. S., Maconnachie, A., Eds.; NATO Advanced Study Institute Series E 89; Martinus Nijhoff Publishers: Hingham, MA, 1985; p 89. (c) Ougizawa, T.; Inoue, T.; Kammer, H. W. *Macromolecules* **1985**, *18*, 2089. (d) Ougizawa, T.; Inoue, T. *Polym. J.* **1986**, *18*, 521. (e) Zacharius, S. L.; ten Brinke, G.; MacKnight, W. J.; Karasz, F. E. *Macromolecules* **1983**, *16*, 381. (f) Roe, R. J.; Zin, W. C. *Macromolecules* **1980**, *13*, 1221. (g) Cong, G.; Huang, Y.; MacKnight, W. J.; Karasz, F. E. *Macromolecules* **1986**, *19*, 2765.
(48) See ref 42, Chapter 6.
(49) (a) Painter, P. C.; Park, Y.; Coleman, M. M. *Macromolecules* **1988**, *21*, 66; **1989**, *22*, 570; **1989**, *22*, 580. (b) Lee, Y. J.; Painter, P. C.; Coleman, M. M. *Macromolecules* **1988**, *21*, 346. (c) Coleman, M. M.; Lichkus, A. M.; Painter, P. C. *Macromolecules* **1989**, *22*, 586. (d) Coleman, M. M.; Jiangbin, H.; Park, Y.; Painter, P. C. *Polymer* **1988**, *29*, 1659. (e) Coleman, M. M.; Lee, Y. J.; Serman, C. J.; Wang, Z.; Painter, P. C. *Polymer* **1989**, *30*, 1298.
(50) (a) Walker, J. S.; Vause, C. A. *J. Chem. Phys.* **1983**, *79*, 2660. (b) ten Brinke, G.; Karasz, F. E. *Macromolecules* **1984**, *17*, 815. (c) Walker, J. S.; Vause, C. A. *Proc. Symp. Thermophys. Prop.* **1982**, *8*, 411.
(51) Modell, M.; Reid, R. C. *Thermodynamics and its Applications*; Prentice-Hall Inc.: Englewood Cliffs, NJ, 1974.
(52) (a) Flory, P. J.; Orwoll, R. A.; Vrij, A. *J. Am. Chem. Soc.* **1964**, *86*, 3507. (b) Rostami, S.; Walsh, D. J. *Macromolecules* **1984**, *17*, 315. (c) Panayiotou, C. G. *Macromolecules* **1987**, *20*, 861. Simha, R. *Macromolecules* **1977**, *10*, 1025. (e) Patterson, D.; Robard, A. *Macromolecules* **1978**, *11*, 690.
(53) Sanchez, I. C. In *Polymer Compatibility and Incompatibility: Principles and Practices*; Solc, K., Ed.; MMI Symposium Series; Harwood: New York, 1982; Vol. 3.
(54) (a) van Krevelen, D. W. *Properties of Polymers*; Elsevier Science Publishing Co.: New York, NY, 1976. (b) Fredenslund, A.; Gmehling, J.; Rasmussen, P. *Vapor–Liquid Equilibrium using UNIFAC*; Elsevier Science Publishing Co.: 1977.
(55) Bernstein, R. E.; Cruz, C. A.; Paul, D. R.; Barlow, J. W. *Macromolecules* **1977**, *10*, 681.
(56) See ref 42, Chapter 9.
(57) Gilmour, I. W.; Hay, J. N. *Polymer* **1977**, *18*, 283.
(58) (a) Hsu, C. C.; Prausnitz, J. M. *Macromolecules* **1974**, *7*, 320. (b) Zeman, L.; Patterson, D. *Macromolecules* **1972**, *5*, 513. (c) Robard, A.; Patterson, D.; Delmas, G. *Macromolecules* **1977**, *10*, 706.
(59) Nishimoto, M.; Keskkula, H.; Paul, D. R. *Polymer*, in press.
(60) Lyngaae-Jorgenson, J.; Sondergaard, K. *Polym. Eng. Sci.* **1987**, *27*, 344, 351.
(61) Nishimoto, M.; Keskkula, H.; Paul, D. R. *Polymer* **1989**, *30*, 1279.

Registry No. SMA (copolymer), 9011-13-6; SAN (copolymer), 9003-54-7; PMMA (homopolymer), 9011-14-7; MAN (copolymer), 30396-85-1; poly(ethyl methacrylate) (homopolymer), 9003-42-3.